ENVIRONMENTAL ASPECTS OF THE SUSTAINED-LOAD CRACKING IN A MILL ANNEALED TITANIUM ALLOY

Y. N. Lenets*, A. H. Rosenberger** and T. Nicholas**

Fatigue pre-cracked compact tension specimens of a mill annealed titanium alloy were subjected to sustained-load cracking in vacuum using several different loading patterns. Three crack propagation stages were distinguished under the constant load regime in respect to the crack front shape across the specimen thickness. Individual unloading cycles (up to 100% of initial load) were shown to have no influence on the crack propagation behavior under otherwise constant load. Good agreement was obtained for data generated under increasing and decreasing stress intensity. The agreement deteriorated close to the sustained-load cracking threshold and was substantially violated by switching from one pattern to another. The crack length effect on the crack behavior under sustained load, earlier reported for laboratory air environment, was confirmed (although at lesser extent) in vacuum. Environmental sensitivity of the sustained-load cracking phenomenon is considered in terms of threshold stress intensity for "no growth - growth" transition as well as crack propagation velocity in laboratory air and vacuum.

INTRODUCTION

A consistent time-dependent degradation in load-carrying capability of some Ti-alloys (see, for example, Meyn (1) and Williams (2)) resulting in subcritical crack extension and ultimately leading to catastrophic fracture under constant applied load *in ambient air or vacuum* is usually referred to as sustained-load cracking (SLC) so as to distinguish the phenomenon from stress-corrosion cracking occurring *in aggressive environments*. Some observations on the SLC in Ti-6Al-4V forging material tested in laboratory air were recently reported by Lenets et al (3). The present paper contains further data for the same material tested in vacuum as well as relevant comparisons and discussion pertaining to the both sets of experimental results.

MATERIAL, SPECIMENS AND TEST TECHNIQUE

A duplex microstructure of mill annealed Ti-6Al-4V alloy (Figure 1) shows elongated β-phase (aspect ratio of 4) with an average grain size between 5 and 40 μm as well as more dispersed α-phase distributed primarily at the β-phase grain boundaries. Compact tension specimens of 5 mm thickness were machined from a round forging in

* SYSTRAN Corporation, 4126 Linden Avenue, Dayton, OH 45432-3068, USA
**Materials and Manufacturing Directorate, Air Force Research Laboratory (AFRL/MLLN), Wright-Patterson Air Force Base, OH 45433-7817, USA

the C-L orientation so as to provide crack growth along Z-axis in Figure 1, which is believed to represent the worse-case condition. The tests were conducted in a vacuum chamber at a pressure not higher than 4.0×10^{-6} Pa using a servohydraulic MTS load frame equipped with a 25 kN load cell. Crack advance during the test was monitored continuously via direct current electric potential (DCEP) technique providing a sensitivity better than 10 μm as well as by periodic optical measurements. An optical microscope was also used for post fracture crack length measurements through the specimen thickness and the DCEP data verification. All specimens were fatigue pre-cracked at R = 0.1 and constant stress intensity K_{max} = 15 MPa$\sqrt{m}$. The SLC tests were conducted under constant load with or without periodic unloading as well as under load shedding while maintaining constant stress intensity (rather than constant load) within each loading step. An intermittent cyclic loading sequence was used to extend the crack for at least 1 mm by fatigue between individual SLC tests. In order to eliminate load history effects, the value of K_{max} used for fatigue crack propagation between individual SLC tests never exceeded 65% of the initial K of the SLC test itself. The cyclic load frequency was 30 Hz and the load ramp velocity at the beginning of the SLC tests was 500 N/s. Additional experimental details are available from (3).

RESULTS AND DISCUSSION

In Figure 2, some of the loading patterns employed in the present study are depicted. In the first case (Figure 2a) the complete test was executed under load control and the hold periods at minimum load during unloading stage of the test were equal to 1 min. The results obtained under constant load that produced an initial stress intensity of 28.5 MPa$\sqrt{m}$ as well as under constant load with periodic unloading of different magnitude are shown in Figures 3a and 3b, respectively. Three stages of the SLC behavior can be distinguished in Figure 3a with respect to the crack front evolution as reflected by a comparison between optical and DCEP crack length measurements. Initially (stage I) the SLC occurred exclusively in the interior of the specimen so that crack front curvature increased. When the difference between an average crack length and that on a surface exceeded 0.6 mm, surface crack propagation commenced and the crack front curvature slightly decreased (stage II). Finally (stage III), after the crack had advanced for more than 1 mm (according to the DCEP measurements), SLC behavior along the entire crack front stabilized with an average difference between DCEP and optical crack length of about 0.5 mm. It should be noted that qualitatively similar behavior resulting in significant crack tunneling was observed during SLC tests in laboratory air (3). However, due to the limited crack extension allowed during SLC, the results from (3) were confined mostly to the stage I as shown in Figure 3a.

At least two factors may significantly influence crack shape development at the beginning of a SLC test. The first is a transition from cyclic (fatigue) to monotonic (SLC) fracture mechanism, while the second factor is a sudden increase in applied load. In the following, an attempt to evaluate the relative importance of these two factors is described. After the crack had propagated about 1.5 mm under stabilized conditions (i.e. since the beginning of the stage III), the load was decreased by 25%, held for 1 min and then restored to its previous value. Subsequently, two more unloading cycles (50% and 100%) were applied as shown schematically in the right hand part of Figure 2a. According to the data collected during this part of the test (Figure 3b), none of these unloading cycles had any noticeable effect on subsequent crack propagation behavior. Small jumps in the crack length immediately after unloading were probably caused by accelerated crack extension during a rising portion of the unloading cycle. An excellent correspondence between optical and DCEP crack length data shows that during this part of the test an even crack front advance occurred. It may, therefore, be postulated that the crack front evolution observed at the beginning of the test (stage I

in Figure 3a) is attributable to the initial crack front shape characteristic of a fatigue crack growth mechanism rather than to a sudden change in load conditions.

Another loading pattern (Figure 2b) employed in the present study was also initiated under load control. However, after the crack behavior had stabilized, the test was switched to stress intensity control and gradual load shedding in 1 MPa$\sqrt{m}$ increments starting from K = 39 MPa$\sqrt{m}$ was executed (see right hand part of Figure 2b) until complete crack arrest. The results of this test, based on the DCEP measurements only, are shown in Figure 4. Good agreement between data points generated under constant load conditions (increasing K) and load shedding (decreasing K) can be seen for an intermediate portion of the curves. At the both ends, however, the situation is quite different. A transition from constant load to load shedding resulted in noticeable decrease in the crack growth rate (upper right end in Figure 4) which from then on demonstrated rather weak dependence on K. It was only after the crack grew more then 1 mm under load shedding conditions that the previous dependence between crack growth rate and applied K was restored and both curves came together. Subsequently the crack growth rate decreased rapidly with stress intensity until complete crack arrest occurred at K = 25 MPa$\sqrt{m}$. One may surmise that the discrepancy between the results furnished by the two loading conditions at lower K values (K < 30 MPa$\sqrt{m}$) should be, at least partially, related to the crack front shape: initially, constant load was applied to a relatively straight crack front remaining after fatigue pre-cracking, while load shedding (especially at K < 30 MPa$\sqrt{m}$) was applied to an extensively curved crack front formed by SLC. Such an explanation, however, does not apply to the transition "constant load - load shedding" (upper right end in Figure 4) when the crack front was already curved by previous SLC. Furthermore, the results pertaining to the unloading tests (see Figures 2a and 3b) do not suggest any substantial influence of the small load change (required by load shedding procedure) on the crack front evolution in the material under consideration.

In both constant load tests shown in Figures 3a and 4, the initial K applied to the fatigue pre-crack was high enough to maintain continuous crack propagation by the SLC mechanism. In other words, the SLC threshold has been exceeded at the beginning of these tests. Figure 5 presents the results of our attempt to evaluate a "no growth - growth" transition in the SLC behavior. This test was also conducted under constant load control, however the initial stress intensity applied to the fatigue pre-crack (K_{init} = 26 MPa$\sqrt{m}$) was only slightly higher than the "no growth" conditions as established by the load shedding test (see Figure 4). As could be seen in Figure 5, minute crack extension of about 0.1 mm occurred at the initial stage of this test (a_{init} = 5.0 mm) after which the crack remained dormant. After 200 min, the SLC test was terminated, the crack was extended by fatigue for more than 1 mm and another SLC test was initiated at K_{init} = 26 MPa$\sqrt{m}$ and a_{init} = 6.3 mm. In this case the crack advanced for more than 0.2 mm before complete arrest. Subsequent SLC test conducted at the same K_{init} and a_{init} = 7.6 mm also resulted in crack arrest after almost 0.5 mm of subcritical crack length increment. However, when the K_{init} = 26 MPa$\sqrt{m}$ was applied to a fatigue pre-crack of 10.2 mm, continuous crack propagation via SLC mechanism occurred until final fracture of the specimen. Such results, reflecting a crack length dependence of the SLC threshold, are consistent with earlier observed behavior of the same material in laboratory air (3). At the same time, the threshold stress intensity corresponding to the onset of continuous SLC in mill annealed Ti-6Al-4V titanium alloy appears to be somewhat higher for vacuum (26 MPa$\sqrt{m}$) as compared to the laboratory air environment (23 MPa$\sqrt{m}$). Another difference between the two environments pertains to the extent of subcritical crack propagation during the near-threshold SLC tests. In vacuum (see Figure 5), the last crack arrest occurred after an increment of about 0.5 mm which corresponds to the upper limit of stage I as shown in Figure 3a. In contrast, the maximum crack increment preceding the last crack arrest in laboratory air was only slightly higher than 0.1 mm (3).

In Figure 6, crack propagation behavior under SLC is compared for both laboratory air (3) and vacuum (present study) in terms of crack growth rate as a function of applied stress intensity. The data available for both environments were intentionally grouped so as to cover two substantially different crack length ranges (5.0...6.5 mm and 11.0...12.5 mm). It would appear that for the rather narrow stress intensity range studied, crack length itself has an adverse effect on the material's resistance against the SLC. Almost a two-fold increase in crack growth rate was noticed for laboratory air environment as a result of initial crack length increase from 5.0...6.5 mm to 11.0...12.5 mm (3). In vacuum, a comparable increase in crack length from 5.1 mm to 11.8 mm also resulted in higher crack growth rates under the same stress intensities (see Figure 6), however the extent of this degrading effect was somewhat lower. Another interesting point is the influence of environment itself which appears to have an ambiguous character. For both crack length intervals studied, a cross-over of the crack growth curves plotted for both environments was observed for K values between 29 and 30 MPa$\sqrt{m}$. At K > 30 MPa$\sqrt{m}$, the crack growth rates in vacuum were lower than those in laboratory air irrespective of the initial crack length. This is in accordance with generally accepted understanding of environmental influence on the crack growth behavior as well as with another finding of the present study (see Figure 5) showing a higher "no growth - growth" threshold for the SLC in vacuum. At the same time, for K < 29 MPa$\sqrt{m}$ the crack growth rates in vacuum appear to be higher than in air. At this time, there is not enough data available to explain such behavior, however the underlying mechanism of the phenomenon may be the same as that causing noticeable difference in the extent of subcritical crack propagation observed during the near-threshold SLC tests in two environments (Figure 5).

SUMMARY

Testing in vacuum environment did not eliminate the sustained-load cracking phenomenon in mill annealed Ti-6Al-4V titanium alloy forging material, supporting therefore an assumption in (3) about the decisive role of internal hydrogen. Another possible mechanism that does not depend on environment is low temperature creep earlier documented for the material under consideration (4). Transition from laboratory air to vacuum was shown to have an ambiguous influence on crack propagation, accelerating the process at K < 29 MPa$\sqrt{m}$ and decelerating it at K > 30 MPa$\sqrt{m}$. At the same time, vacuum slightly increased "no growth - growth" threshold stress intensity for sustained-load cracking in the tested material.

REFERENCES

(1) Williams, D. N., Met. Trans., Vol. 4, 1973, pp. 675-680.

(2) Meyn, D. A., Met. Trans., Vol. 5A, 1974, pp. 2405-2414.

(3) Lenets, Y., Thomas, J. P. and Nicholas, T., "Sustained-load cracking in mill annealed Ti-6Al-4V at room temperature", Proceedings of the ASME Conference on "Recent Advances in Solids/Structures and Applications of Metallic Materials". Edited by Y. W. Kwon, D. C. Davis, H. H. Chung and L. Librescu. ASME International, New York, 1997, pp. 315-321.

(4) Morrissey, R. J., Frequency and mean stress effects in high cycle fatigue of Ti-6Al-4V", MS Thesis, Georgia Institute of Technology, Atlanta, GA, 1997.

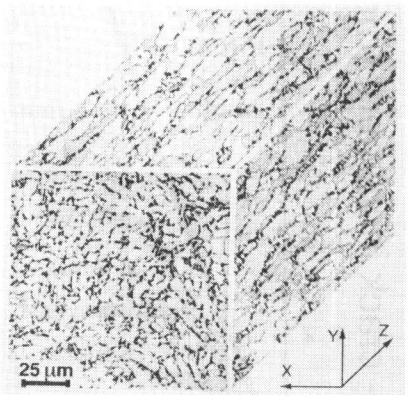

Figure 1. Microstructure of the material

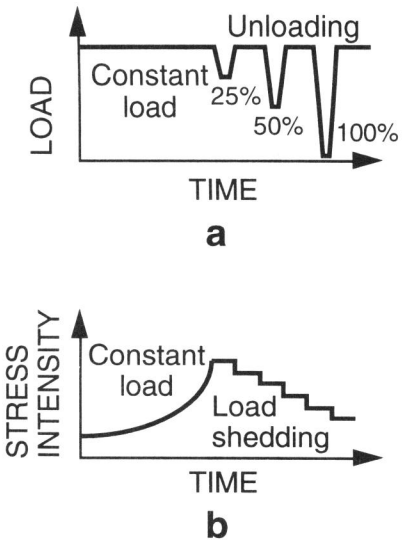

Figure 2. Load patterns used

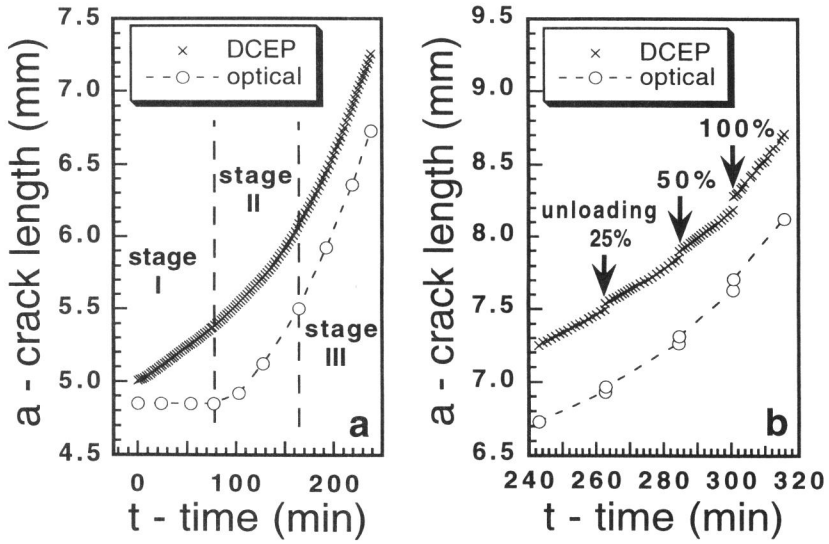

Figure 3. The SLC behavior (a) without and (b) with periodic unloading under the load pattern shown in Figure 2a. Note different scale along abscissa

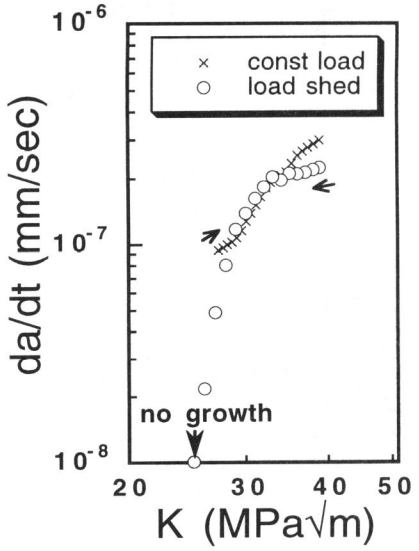

Figure 4. The SLC behavior under the load pattern shown in Figure 2b

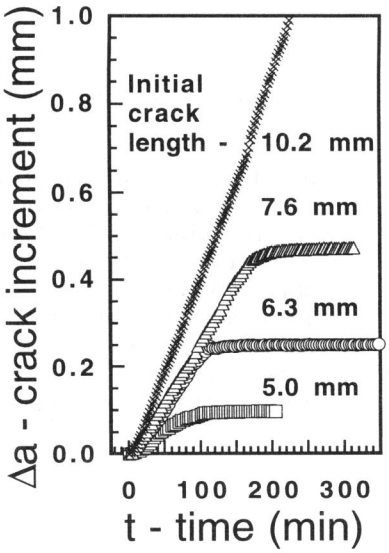

Figure 5. "No growth - growth" threshold test results

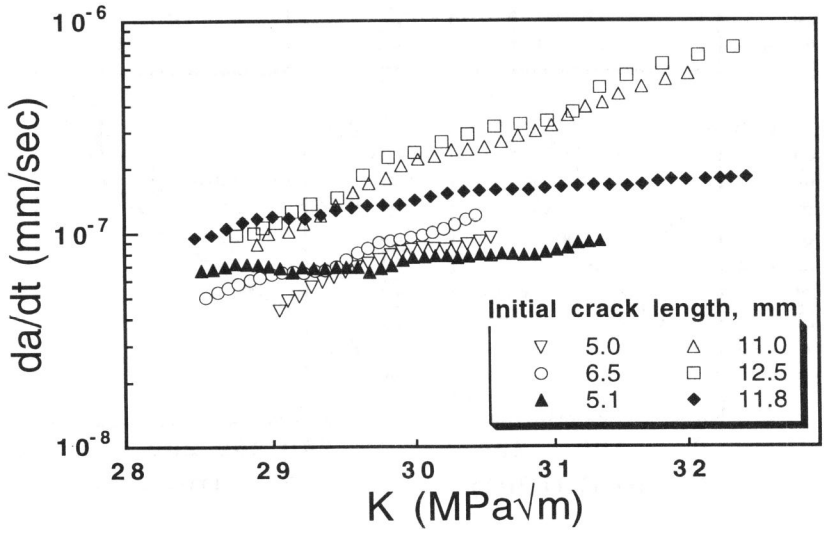

Figure 6. SLC behavior in laboratory air (open symbols) and vacuum (closed symbols)